2024 European Control Conference (ECC)
June 25-28, 2024. Stockholm, Sweden

A Nonlinear Negative-Imaginary Systems Framework with Actuator Saturation for Control of Electrical Power Systems

Yijun Chen[1], Kanghong Shi[1], Ian R. Petersen[1], and Elizabeth L. Ratnam[1]

Abstract— **In the transition to net zero, it has been suggested that a massive expansion of the electric power grid will be required to support emerging renewable energy zones. In this paper, we propose the use of battery-based feedback control and nonlinear negative-imaginary (NNI) systems theory to reduce the need for such an expansion by enabling the more complete utilization of existing grid infrastructure. By constructing a novel Luré-Postnikov-like Lyapunov function, a stability result is developed for the feedback interconnection of a NNI system and a NNI controller. Additionally, a new class of NNI controllers is proposed to deal with actuator saturation. We show that in this control framework, the controller eventually leaves the saturation boundary, and the feedback system is locally stable in the sense of Lyapunov. This provides theoretical support for the application of battery-based control in electrical power systems. Validation through simulation results for single-machine-infinite-bus power systems supports our results. Our approach has the potential to enable a transmission line to operate at its maximum power capacity, as stability robustness is ensured by the use of a feedback controller.**

I. Introduction

To meet the global challenge of climate change and the rapid transition to net-zero electricity, it has been suggested that a massive expansion of the electric power grid will be required to support emerging renewable energy zones and the electrification of other sectors including transportation. In this paper, we propose the use of battery-based feedback control and nonlinear negative-imaginary systems (NNI) theory [1]–[3] to reduce the need for such an expansion by enabling the more complete utilization of existing grid infrastructure.

Frequency deviations in electric power systems pose risks such as equipment damage, transmission line overloads, and compromised system reliability [4]. Therefore, the primary aim of frequency control is to maintain synchronization with the nominal frequency. Regulating frequency involves managing both the generation and load sides. Automatic generation control, a conventional frequency regulation scheme on the generation side, adjusts generator setpoints in response to frequency variations and unexpected power flows between different areas [4], [5]. However, with the increasing integration of renewable energy sources, the heightened volatility in non-dispatchable renewable generation poses challenges for generator-side control, shifting attention towards load control strategies.

In recent years, advancements in battery technologies have led to the widespread adoption of rechargeable batteries in electric vehicles, the use of large grid storage batteries, and the proliferation of domestic solar-powered batteries [6], [7]. In addition to energy storage supporting local power management, this transformative development may also open the possibility for energy storage systems to actively participate in regulating system frequency and ensuring transient stability in power systems. Nevertheless, integrating distributed energy storage systems into power systems necessitates a profound understanding of the interaction between rapidly controllable batteries and the dynamic behavior of power systems. Considering the possibility of real-time angle measurements for future power systems [8], the work of [9] proposes angle feedback linearization control for power transmission networks using linear negative-imaginary (NI) systems theory [10]–[12] to guarantee transient stability and frequency synchronization. However, it does not take into account actuator saturation, which is of a nonlinear nature. For this reason, it is useful to investigate controllers with actuator saturation in a nonlinear systems framework. In addition, NI system theory [1]–[3] can be utilized to guarantee power system transient stability, ensure power system robustness, and address consensus problems relating to the convergence of bus angles.

Therefore, this paper proposes a NNI systems framework with actuator saturation for control of electrical power systems. From the technical point of view, our contributions are two-fold: 1) we constructed a novel candidate Lyapunov function, fashioned in a manner reminiscent of the Luré-Postnikov form [13] and intended for stability proofs for feedback interconnection of NNI systems; 2) we propose a new class of NNI controllers to deal with actuator saturation and ensure system stability. Moreover, our technical results provide theoretical support for applications in the field of electrical power systems. Our contributions to the area of electrical power systems are two-fold: 1) in the absence of a controller, we analyze the invariant set of the single-machine-infinite-bus (SMIB) power systems, which serves as a theoretical foundation for the stability condition arising from the well-known equal area criterion [5]; 2) we present a control framework using real-time angle sensors and large-scale batteries as actuators with saturation, which exhibits the ability to enhance power system transient stability without the need for over-engineering.

This paper is organized as follows: Section II provides preliminary knowledge on the definition of NNI systems. Section III provides the stability results for the feedback

[1]The School of Engineering, The Australian National University, Canberra, Australia, emails: {yijun.chen, kanghong.shi, ian.petersen, elizabeth.ratnam }@anu.edu.au.

This work was supported by the Australian Research Council under grants DP230102443 and LP210200473.

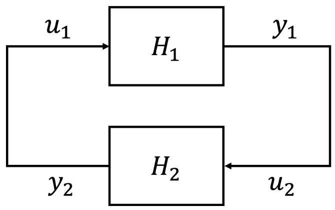

Fig. 1: Feedback interconnection of two systems H_1 and H_2.

interconnection of NNI systems. Section IV proposes a NNI systems framework with actuator saturation for control. Sections V and VI present the application to SMIB systems. In Section VII, simulation results are given. Section VIII concludes the paper.

II. Preliminaries

In this section, we introduce the definition of NI property for nonlinear systems.

Consider a single-input-single-output (SISO) nonlinear system with the following state-space model:

$$\dot{x} = f(x, u), \tag{1a}$$
$$y = h(x, u), \tag{1b}$$

where $x \in \mathbb{R}^n$ is the state, $u \in \mathbb{R}$ is the input, $y \in \mathbb{R}$ is the output, $f : \mathbb{R}^n \times \mathbb{R} \to \mathbb{R}^n$ is a Lipschitz continuous function, and $h : \mathbb{R}^n \times \mathbb{R} \to \mathbb{R}$ is a class C^1 function.

Assumption 1: Without loss of generality, assume $(x^*, u^*) = (0, 0)$ is an equilibrium point of the system (1); i.e., $f(0, 0) \equiv 0$. Moreover, assume the output at the equilibrium $(0, 0)$ is $y^* = h(0, 0) \equiv 0$.

Definition 1: The system (1) is said to be a nonlinear negative-imaginary (NNI) system if there exists a positive semidefinite storage function $V : \mathbb{R}^n \to \mathbb{R}$ of class C^1 such that for all $t \geq 0$,

$$\dot{V}(x) \leq \int_0^u \frac{\partial}{\partial x} h(x, \xi) \dot{x} d\xi. \tag{2}$$

III. Feedback Interconnection of NNI Systems

Consider a SISO NNI system H_1:

$$H_1 : \quad \dot{x}_1 = f_1(x_1, u_1), \tag{3a}$$
$$y_1 = h_1(x_1), \tag{3b}$$

where $x_1 \in \mathbb{R}^{n_1}$ is the state, $u_1 \in \mathbb{R}$ is the input, $y_1 \in \mathbb{R}$ is the output, $f_1 : \mathbb{R}^{n_1} \times \mathbb{R} \to \mathbb{R}^{n_1}$ is a Lipschitz continuous function, and $h_1 : \mathbb{R}^{n_1} \times \mathbb{R} \to \mathbb{R}$ is a class C^1 function.

Also consider a SISO NNI system H_2:

$$H_2 : \quad \dot{x}_2 = f_2(x_2, u_2), \tag{4a}$$
$$y_2 = h_2(x_2, u_2), \tag{4b}$$

where $x_2 \in \mathbb{R}^{n_2}$ is the state, $u_2 \in \mathbb{R}$ is the input, $y_2 \in \mathbb{R}$ is the output, $f_2 : \mathbb{R}^{n_2} \times \mathbb{R} \to \mathbb{R}^{n_2}$ is a Lipschitz continuous function, and $h_2 : \mathbb{R}^{n_2} \times \mathbb{R} \to \mathbb{R}$ is a class C^1 function.

Further consider the feedback interconnection of two systems H_1 and H_2 as shown in Fig. 1. The relation between the inputs and the outputs is described by $y_1 \equiv u_2$ and $y_2 \equiv u_1$.

We define a candidate Lyapunov function of the feedback system (H_1, H_2) as

$$W(x_1, x_2) = V_1(x_1) + V_2(x_2) - \int_0^{h_1(x_1)} h_2(x_2, \xi) d\xi. \tag{5}$$

Assumption 2: Suppose there exists a compact domain $\mathcal{D} \subset \mathbb{R}^{n_1} \times \mathbb{R}^{n_2}$ such that $(0, 0) \in \mathcal{D}$ and $W(x_1, x_2) > 0$ for $(x_1, x_2) \in \mathcal{D} \setminus \{(0, 0)\}$.

Remark 1: We have constructed a novel candidate Lyapunov function (5), fashioned in a manner reminiscent of the Luré-Postnikov Lyapunov function [13]. This form points to an interesting connection between NNI systems theory and the Popov stability condition [13]; see also [14].

In the following theorem, we prove that the equilibrium $(x_1^*, x_2^*) = (0, 0)$ of the feedback system (H_1, H_2) is locally stable in the sense of Lyapunov.

Theorem 1: Suppose Assumption 1 and Assumption 2 hold. Then, the equilibrium $(x_1^*, x_2^*) = (0, 0)$ of the feedback system (H_1, H_2) is locally stable in the sense of Lyapunov.
Proof. The proof can be found in [15]. □

IV. Feedback Interconnection of Saturated NNI Systems

Consider two SISO NNI systems H_1 and H_3. The system H_1 is described by the state-space model (3). Simultaneously, the system H_3 is characterized by:

$$H_3 : \quad \dot{x}_3 = f_3(x_3, u_3), \tag{6a}$$
$$y_3 = h_3(x_3) - L u_3, \tag{6b}$$

where $L \in \mathbb{R}$, $x_3 \in \mathbb{R}^{n_3}$ is the state, $u_3 \in \mathbb{R}$ is the input, $y_3 \in \mathbb{R}$ is the output, $f_3 : \mathbb{R}^{n_3} \times \mathbb{R} \to \mathbb{R}^{n_3}$ is a Lipschitz continuous function, and $h_3 : \mathbb{R}^{n_3} \to \mathbb{R}$ is a class C^1 function.

Suppose both systems H_1 and H_3 are NNI. Consequently, according to Definition 1, for the system H_1, there exists a positive semidefinite storage function $V_1(x_1) \geq 0$ with $V_1(0) = 0$, satisfying that

$$\dot{V}_1(x_1) \leq u_1 \dot{h}_1(x_1), \forall x_1, u_1.$$

Also, for the system H_3, there exists a positive semidefinite storage function $V_3(x_3) \geq 0$ with $V_3(0) = 0$, satisfying that

$$\dot{V}_3(x_3) \leq \int_0^{u_3} \frac{\partial (h_3(x_3) - L\xi)}{\partial x_3} \dot{x}_3 d\xi = u_3 \dot{h}_3(x_3), \forall x_3, u_3.$$

A. Saturated NNI Systems

Consider the feedback system (H_1, H_3). Typically, it can be interpreted as H_1 being the plant and H_3 being the controller. However, in practical implementation, the actuator for the controller H_3 may be subject to saturation. As a result, we further consider an anti-windup compensator system to address potential issues that may arise from saturation. In particular, we consider a situation in which the controller H_3 is to replace a nominal nonlinear feedback $g(u_3)$ via feedback linearization; see also [9]. Then in the presence of actuator saturation, we consider the controller

$$\hat{H}_3 :\ \dot{\hat{x}}_3 = \begin{cases} f_3(\hat{x}_3, \hat{u}_3), & |h_3(\hat{x}_3) - L\hat{u}_3 - g(\hat{u}_3)| < b, \\ -\alpha \frac{\partial V_3(\hat{x}_3)^\top}{\partial \hat{x}_3}, & |h_3(\hat{x}_3) - L\hat{u}_3 - g(\hat{u}_3)| \geq b, \end{cases} \tag{7a}$$

$$\begin{aligned} \hat{y}_3 &= \hat{h}_3(\hat{x}_3, \hat{u}_3) \\ &= g(\hat{u}_3) + \text{sat}_b(h_3(\hat{x}_3) - L\hat{u}_3 - g(\hat{u}_3)), \end{aligned} \tag{7b}$$

where $\alpha > 0$ is a design choice, $b \geq 0$ is the saturation parameter, and $g : \mathbb{R} \to \mathbb{R}$ is a class C^1 function such that $|L\hat{u}_3 + g(\hat{u}_3)| < b$ for $\hat{u}_3 \in \mathcal{D}_{\hat{u}_3}$. The domain $\mathcal{D}_{\hat{u}_3}$ represents the domain of interest for the output of the system H_1. For example, in power systems, $\mathcal{D}_{\hat{u}_3}$ is the domain of attraction for rotor angles. Here, $\text{sat}_b(w)$ represents the saturation function

$$\text{sat}_b(w) = \begin{cases} -b, & w \leq -b, \\ w, & -b < w < b, \\ b, & w \geq b, \end{cases}$$

where the saturation variable w is defined to be $w = h_3(\hat{x}_3) - L\hat{u}_3 - g(\hat{u}_3)$.

Remark 2: When $g(\hat{u}_3) \equiv 0$, the output (7b) in the system $\hat{H}_3$ reduces to $\hat{y}_3 = \text{sat}_b(h_3(\hat{x}_3) - L\hat{u}_3) = \text{sat}_b(y_3)$, characterizing actuator saturation of the output (6b) in the system H_3. To ensure the applicability of our theory to power systems, we propose the more general form (7b) for the controller $\hat{H}_3$ to replace a nominal nonlinear feedback $g(\hat{u}_3)$ via feedback linearization in which $g(\hat{u}_3)$ represents the sine function applied to the rotor angle as detailed in Section VI.

As shown in the following Theorem 2 and Remark 3, the advantages of such a control design for the controller $\hat{H}_3$ are two-fold: (1) it ensures that the controller $\hat{H}_3$ maintains NNI property, (2) and it ensures that the actuator does not stay at the saturation boundary as time goes to infinity.

Theorem 2: The controller $\hat{H}_3$ is NNI.
Proof. The proof can be found in [15]. □

Remark 3: It is noted that the definition of the system $\hat{H}_3$ ensures that the actuator does not stay at the saturation boundary as time goes to infinity. For all

$$\hat{x}_3 \in \mathcal{D}_{sat} = \{\hat{x}_3 : |w| \geq b\},$$

we have $\dot{V}_3(\hat{x}_3) = -\alpha \| \frac{\partial V_3(\hat{x}_3)}{\partial \hat{x}_3} \|^2 < 0$, which implies that $V_3(\hat{x}_3)$ will keep decreasing when $\hat{x}_3 \in \mathcal{D}_{sat}$. Since $V_3(0) = 0$, $h_3(0)$, $|L\hat{u}_3 + g(\hat{u}_3)| < b$, and the functions $V_3(\cdot)$ and $h_3(\cdot)$ are continuous, it follows that $\hat{x}_3$ will eventually leave the saturation region $\mathcal{D}_{sat}$.

B. Lyapunov Stability of the Feedback Interconnection

Consider the feedback system $(H_1, \hat{H}_3)$, where the systems H_1 and H_3 are assumed to be NNI and the system $\hat{H}_3$ can be proved to be NNI by applying Theorem 2. As in Eq. (5), a candidate Lyapunov function for the feedback system $(H_1, \hat{H}_3)$ is chosen as

$$\hat{W}(x_1, \hat{x}_3) = V_1(x_1) + V_3(\hat{x}_3) - \int_0^{h_1(x_1)} \hat{h}_3(\hat{x}_3, \xi) d\xi.$$

Assumption 3: Suppose there exists a compact domain $\mathcal{D} \subset \mathbb{R}^{n_1} \times \mathbb{R}^{n_3}$ such that $(0,0) \in \mathcal{D}$ and $\hat{W}(x_1, \hat{x}_3) > 0$ for $(x_1, \hat{x}_3) \in \mathcal{D} \setminus \{(0,0)\}$.

In the following theorem, we show that the equilibrium $(x_1^*, \hat{x}_3^*) = (0,0)$ of the feedback system $(H_1, \hat{H}_3)$ is locally stable in the sense of Lyapunov.

Theorem 3: Suppose Assumption 1 and Assumption 2 hold. Then, the equilibrium $(x_1^*, \hat{x}_3^*) = (0,0)$ of the feedback system $(H_1, \hat{H}_3)$ is locally stable in the sense of Lyapunov.
Proof. The proof can be found in [15]. □

V. Single-Machine-Infinite-Bus Power Systems

Consider a single-machine-infinite-bus (SMIB) power system. A generator is connected to an infinite bus representing the bulk power grid. For the infinite bus, the voltage magnitude $|V_s|$ is assumed to be constant and the voltage phase is assumed to be zero. For the generator bus, we denote the rotor angle in the stationary reference frame by θ, the rotor speed by ω, and the nominal frequency by ω^0. Then, the voltage at time t is written as a cosine function multiplied by its voltage magnitude $|V_g|$:

$$\begin{aligned} |V_g| \cos(\theta(t)) &= |V_g| \cos(\omega^0 t + \delta(t)) \\ &= |V_g| \cos(\omega^0 t + \bar{\delta} + \tilde{\delta}(t)), \end{aligned}$$

where $\delta(t)$ represents the voltage phase angle, $\bar{\delta}$ represents the voltage phase angle at steady state, and $\tilde{\delta}(t) = \delta(t) - \bar{\delta}$ represents the voltage phase angle deviation. The frequency on the generator bus is defined as

$$\omega = \dot{\theta} = \omega^0 + \dot{\tilde{\delta}}.$$

Based on the generator mechanical model [5], the swing equation of the generator bus is described by

$$M\ddot{\delta} = P^M - P^E - D\dot{\delta}, \tag{8}$$

where $M = \frac{2H}{\omega^0} > 0$ represents inertia on the generator bus with a lumped parameter $H > 0$, and $D \geq 0$ is the damping coefficient. Here, P^M represents the mechanical power injection on the generator bus, and P^E represents the electric power output of the generator bus. The electric power output P^E of the generator bus is given by

$$P^E = \frac{|V_g||V_s|}{X} \sin\delta = P^E_{\max} \sin\delta, \tag{9}$$

where X is the total reactance, and $P^E_{\max}$ is the maximum power transfer between the generator bus and the infinite bus, and $|V_g|$ and $|V_s|$ are at the nominal voltage.

Fault Setting. In practice, sudden changes in electrical or mechanical power can arise. Prior to a fault occurrence, the SMIB system (8) is assumed to be at a stable equilibrium given by $(\bar{\delta}, \bar{P}^M, \bar{P}^E_{\max})$, where it satisfies the relation $\bar{P}^M = \bar{P}^E_{\max} \sin\bar{\delta}$. In the aftermath of a fault, the generator bus frequency deviates from its nominal value ω^0. The phase angle deviates from its steady-state value $\bar{\delta}$ and may reach a new steady-state value δ_0 caused by sudden changes in mechanical or electrical power. In this paper, we specifically

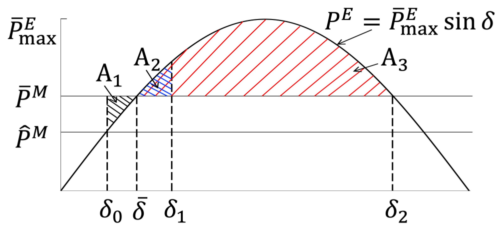

Fig. 2: Mechanical power and electrical power versus angle.

focus on the post-fault transient stability, during which the mechanical power and maximum power transfer return to their pre-fault values $(\bar{P}^M, \bar{P}^E_{\max})$.

A. Equal Area Criterion

In what follows, we present the equal area criterion, a direct method for determining post-fault transient stability for SMIB systems without damping [5].

Consider a scenario where a fault occurs leading to a change in mechanical power while the maximum power transfer remains unaffected. Denote the mechanical power during the fault as $\hat{P}^M$. Assume that the phase angle stabilizes at a steady-state value δ_0 shortly before the fault is resolved. Subsequently, after the fault is cleared, the mechanical power returns to its pre-fault value $\bar{P}^M$. We illustrate the mechanical power and electrical power versus power angle in Fig. 2.

Starting from initial angle δ_0, the angle accelerates and δ increases. When δ reaches $\bar{\delta}$, $\dot{\delta}$ is still positive and δ continues to increase with a decreasing speed. Eventually, δ reaches a maximum value δ_1 and swings back toward $\bar{\delta}$.

The equal area criterion states that the accelerating area must be equal to the decelerating area, i.e., $A_1 = A_2$. It is noted that δ_1 cannot exceed $\delta_2 = \pi - \bar{\delta}$. Otherwise, the mechanical power injection would exceed the electric power output and the generator bus would accelerate again, leading to a further increase in δ and loss of stability. In other words, the system can maintain stability around $\bar{\delta}$, if $A_1 - A_3 < 0$, equivalently,

$$(\pi - \bar{\delta} - \delta_0)\sin\bar{\delta} - \cos\bar{\delta} - \cos\delta_0 < 0. \tag{10}$$

B. Lyapunov Stability of SMIB Systems

In what follows, we show that the SMIB system is locally stable in the sense of Lyapunov.

The swing equation of the SMIB system can be rewritten in terms of the angle deviation $\tilde{\delta}$ specifically:

$$M\ddot{\tilde{\delta}} + D\dot{\tilde{\delta}} = \bar{P}^E_{\max}\sin\bar{\delta} - \bar{P}^E_{\max}\sin(\tilde{\delta} + \bar{\delta}), \tag{11}$$

with initial angle deviation $\tilde{\delta}_0 = \delta_0 - \bar{\delta} \neq 0$. By reformulating the system (11) into the feedback interconnection of two NNI systems, we can prove that the SMIB system is locally stable in the sense of Lyapunov.

Define $x_1 = [\dot{\tilde{\delta}}, \tilde{\delta}]^\top \in \mathbb{R}^2$, $u_1 \in \mathbb{R}$, $x_2 \equiv 0$, and $u_2 \in \mathbb{R}$. The system (11) can be represented by the interconnection of two systems:

$$H_1: \quad \dot{x}_1 = Ax_1 + Bu_1 \tag{12a}$$
$$y_1 = Cx_1 \tag{12b}$$
$$H_2: \quad y_2 = \bar{P}^E_{\max}\sin\bar{\delta} - P^E_{\max}\sin(u_2 + \bar{\delta}) \tag{12c}$$

where H_1 has system matrices $A = \begin{bmatrix} \frac{-D}{M} & 0 \\ 1 & 0 \end{bmatrix}$, $B = \begin{bmatrix} \frac{1}{M} \\ 0 \end{bmatrix}$, and $C = \begin{bmatrix} 0 & 1 \end{bmatrix}$.

In the subsequent theorem, establishing the NI nature of both systems lays the ground for proving the local stability of the SMIB system in the sense of Lyapunov.

Theorem 4: In the absence of the damping $(D = 0)$, the equilibrium $(\dot{\tilde{\delta}}^*, \tilde{\delta}^*) = (0, 0)$ of the system (11) is locally stable in the sense of Lyapunov. In the presence of the damping $(D > 0)$, the equilibrium $(\dot{\tilde{\delta}}^*, \tilde{\delta}^*) = (0, 0)$ of the system (11) is locally asymptotically stable.

Proof. The proof can be found in [15]. □

C. Invariant Set

Since the system (11) may have several equilibria, stability is not sufficient to guarantee that the system converges to the equilibrium at $(0, 0)$. We need to find an invariant set so that any initial state starting from the region will remain in this region. An invariant subset of $\mathcal{D}$ is considered as

$$\Omega_c = \{x_1 \in \mathbb{R}^2 | W(x_1) \leq c\}. \tag{13}$$

We find the constant $c > 0$ as follows. Consider the form of the Lyapunov function

$$W(\tilde{\delta}, \dot{\tilde{\delta}}) = \frac{M}{2}\dot{\tilde{\delta}}^2 - \bar{P}^E_{\max}\tilde{\delta}\sin\bar{\delta} + \bar{P}^E_{\max}\cos\bar{\delta} - \bar{P}^E_{\max}\cos(\tilde{\delta} + \bar{\delta}).$$

Since the term $M\dot{\tilde{\delta}}^2$ increase monotonically with $|\dot{\tilde{\delta}}|$, then we only analyze the function

$$\Gamma(\tilde{\delta}) = -\bar{P}^E_{\max}\tilde{\delta}\sin\bar{\delta} + \bar{P}^E_{\max}\cos\bar{\delta} - \bar{P}^E_{\max}\cos(\tilde{\delta} + \bar{\delta}).$$

We take the derivative of $\Gamma(\tilde{\delta})$ with respect to $\tilde{\delta}$:

$$\frac{d}{d\tilde{\delta}}\Gamma(\tilde{\delta}) = -\bar{P}^E_{\max}\sin\bar{\delta} + \bar{P}^E_{\max}\sin(\tilde{\delta} + \bar{\delta}).$$

Letting $\frac{d}{d\tilde{\delta}}\Gamma(\tilde{\delta}) = 0$, we have that $\sin(\tilde{\delta} + \bar{\delta}) = \sin\bar{\delta}$. That is $\tilde{\delta} = 2k\pi$ or $\tilde{\delta} = -2\bar{\delta} + (2k+1)\pi$. We only focus on a neighborhood of the origin. The function $\Gamma(\tilde{\delta})$ has two local maxima near the origin. They are $\Gamma(-\pi - 2\bar{\delta}) = \bar{P}^E_{max}(2\cos(\bar{\delta}) + (\pi - 2\bar{\delta})\sin(\bar{\delta}))$ and $\Gamma(\pi - 2\bar{\delta}) = \bar{P}^E_{max}(2\cos(\bar{\delta}) - (\pi - 2\bar{\delta})\sin(\bar{\delta}))$. Since $\bar{\delta} \in (0, \frac{\pi}{2})$, then $\Gamma(\pi - 2\bar{\delta}) < \Gamma(-\pi - 2\bar{\delta})$. Hence, we have

$$0 < c < \Gamma(\pi - 2\bar{\delta}) = \bar{P}^E_{max}(2\cos(\bar{\delta}) - (\pi - 2\bar{\delta})\sin(\bar{\delta})). \tag{14}$$

Note that the set (13) with (14) may consist several disconnected sets. The one that contains the origin is a subset of $\mathcal{D}$. To restrict the states to this set, we give an extra upper bound on the state $\tilde{\delta}$. Denoting $x_1^{[2]} := \tilde{\delta}$, we have

$$\Omega = \{x_1 \in \mathbb{R}^2 | W(x_1) \leq c \text{ and } |x_1^{[2]}| \leq \pi - 2\bar{\delta}\}, \tag{15}$$

where c is given in (14). Therefore, the set (15) is the required compact invariant set.

Comparison with Equal Area Criterion. Assuming the SMIB system starts at initial state $(\dot{\tilde{\delta}}, \tilde{\delta}) = (\delta_0, 0)$. According to Eq. (15), the invariant set for $\tilde{\delta}_0$ is described by

$$\{\tilde{\delta} : (\pi - 2\bar{\delta} - \tilde{\delta}) \sin\bar{\delta} - \cos\bar{\delta} - \cos(\bar{\delta} + \tilde{\delta}) < 0\}.$$

By shifting $\tilde{\delta}_0$ to $\delta_0 = \bar{\delta} + \tilde{\delta}_0$, the invariant set for δ_0 becomes

$$\{\delta : (\pi - \bar{\delta} - \delta) \sin\bar{\delta} - \cos\bar{\delta} - \cos(\delta) < 0\}, \tag{16}$$

which aligns with the stability condition (10) derived from the equal area criterion. Notably, the stability condition (10) derived from the equal area criterion represents a specific case within our analysis of the invariant set (15), assuming $\dot{\delta}_0 = 0$. Thus, our exploration of the invariant set serves as a theoretical foundation for the equal area criterion from perspective of nonlinear systems theory.

VI. SMIB Systems with Battery-based Control

In what follows, our focus lies in equipping the generator bus with a large-scale battery and providing a systematic method to design angle based feedback control based on the use of the battery-based actuator to enhance the transient stability of SMIB systems.

We consider a battery equipped at the generator bus. Hence, modifying Eq. (8), the swing equation is revised as

$$M\ddot{\delta} = P^M + P^{ST} - P^E - D\dot{\delta}, \tag{17}$$

where P^{ST} represents the power output of the local storage device at the generator bus. It is noted that the battery has a finite maximum power output.

Prior to a fault occurrence, the system (17) is at a stable equilibrium $(\bar{\delta}, \bar{P}^M, \bar{P}^{ST}, \bar{P}^E_{\max})$, where $\bar{P}^M + \bar{P}^{ST} - \bar{P}^E_{\max} \sin\bar{\delta} = 0$. In the aftermath of a fault, the generator bus frequency deviates from its nominal value ω^0. The phase angle deviates from its steady-state value $\bar{\delta}$ and may reach a new stable-state value δ_0 caused by sudden changes in mechanical or electrical power. In what follows, we investigate the post-fault transients, during which mechanical power and maximum power transfer are back to pre-fault values $(\bar{P}^M, \bar{P}^E_{\max})$. We aim to design battery-based angle feedback control to stabilize the SMIB system even when equal area criterion (10) is not satisfied.

A. Angle Feedback Controllers

We define the change in storage power output, $\tilde{P}^{ST} = P^{ST} - \bar{P}^{ST}$, as the difference from the storage power output before a fault occurs. The swing equation of the SMIB system with a local storage device can be rewritten in terms of the angle deviation $\tilde{\delta}$ specifically:

$$M\ddot{\tilde{\delta}} + D\dot{\tilde{\delta}} = \tilde{P}^{ST} + \bar{P}^E_{\max} \sin\bar{\delta} - \bar{P}^E_{\max} \sin(\tilde{\delta} + \bar{\delta}), \tag{18}$$

with initial angle deviation $\tilde{\delta}_0 = \delta_0 - \bar{\delta} \neq 0$.

In what follows, we present a battery-based control framework considering two different actuator scenarios: one without saturation and the other with a saturation.

Battery-based Control without Saturation. Define $x_3 \in \mathbb{R}$ and $u_3 \in \mathbb{R}$. Also define $g(u_3) = \bar{P}^E_{\max} \sin\bar{\delta} - \bar{P}^E_{\max} \sin(u_3 + \bar{\delta})$. The angle feedback controller without actuator saturation is represented by

$$H_3 : \quad \dot{x}_3 = -\frac{1}{\tau} x_3 + \frac{K}{\tau} u_3, \tag{19a}$$

$$y_3 = x_3 - L u_3, \tag{19b}$$

where $\tau > 0, K > 0$, and $L > 0$. Note that this will correspond to a phase-lead compensator.

The following theorem guides us how to select the design choice (K, L).

Theorem 5: Consider the system H_1 with the state-space model (12) and the system H_3 with the state-space model (19). Then, the equilibrium $(x_1^*, x_3^*) = (0, 0, 0)$ of the feedback system (H_1, H_3) is globally asymptotically stable, if $K - L < 0$.

Proof. The proof can be found in [15]. □

Battery-Based Control with Saturation. In practical scenarios, the change in storage power output $\tilde{P}^{ST}$ available for sustaining transient stability is constrained by a saturation parameter $b \geq 0$, i.e., $|\tilde{P}^{ST}| < b$.

Drawing inspiration from Section IV, the form of the angle feedback controller with actuator saturation is given by

$$\hat{H}_3 : \quad \dot{\hat{x}}_3 = \begin{cases} -\frac{1}{\tau}\hat{x}_3 + \frac{K}{\tau}\hat{u}_3, & |\hat{x}_3 - L\hat{u}_3 - g(\hat{u}_3)| < b, \\ -\frac{\alpha}{K}\hat{x}_3, & |\hat{x}_3 - L\hat{u}_3 - g(\hat{u}_3)| \geq b, \end{cases} \tag{20a}$$

$$\hat{y}_3 = g(\hat{u}_3) + \text{sat}_b(\hat{x}_3 - L\hat{u}_3 - g(\hat{u}_3)), \tag{20b}$$

where $\tau > 0$, $K > 0$, $L > 0$ and $\alpha > 0$.

Our following exploration involves two extreme conditions, namely, $b = 0$ and $b = \infty$.

- When $b = 0$: The output of the system $\hat{H}_3$ remains unaffected by the state $\hat{x}_3$, resulting in $\hat{y}_3 = g(\hat{u}_3)$. This scenario corresponds to the absence of a local storage device at the generator bus, without any implemented controller to enhance transient stability. The invariant set is described by the set (15).
- When $b = \infty$: The controller is not subject to saturation, leading to the system $\hat{H}_3$ reducing to the system H_3. Here, the closed-loop system becomes globally asymptotically stable.

Remark 4: For $0 < b < \infty$, the feedback system $(H_1, \hat{H}_3)$ is locally stable in the sense of Lyapunov and the invariant set should be larger than the set (15) by continuity. The analytical estimation of the invariant set for the initial state $(\dot{\tilde{\delta}}_0, \tilde{\delta}_0)$ in the presence of saturation is a complicated task. Hence, we rely on simulations to illustrate the effectiveness of the proposed controller operating with actuator saturation.

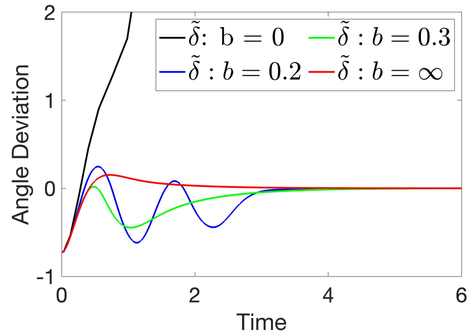

Fig. 3: The angle deviation without a controller $b = 0$ and with controllers under three actuator saturation cases $b \in \{0.2, 0.3, \infty\}$.

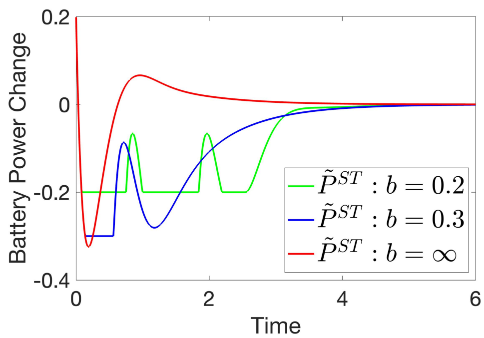

Fig. 4: The trajectories of battery power output change under three actuator saturation cases $b \in \{0.2, 0.3, \infty\}$.

VII. Simulations

Consider an example of a SMIB system from [5] with per-unit settings $H = 4$, $D = 0$, $P^M = 0.8$, and $P^E = 1$. The nominal system frequency is 50Hz and the angle at steady state before the occurrence of a fault is $\bar{\delta} = 0.927$ rad. We then consider the occurrence of a fault that causes a new initial angle $\delta(0) = 0.2$ rad.

Controller Setting. The parameters for the angle feedback controller (20) are set as $\tau = 0.1, K = 1, L = 1.1$, and $\alpha = 1$. We can check that $K - L < 0$. We test three actuator saturation cases $b \in \{0.2, 0.3, \infty\}$.

Simulation Results. In Fig. 3, we plot the angle deviation for the SMIB system without a controller $b = 0$ and with controllers under three actuator saturation cases $b \in \{0.2, 0.3, \infty\}$. Since the stability condition of the equal area condition (10) is not satisfied, the SMIB system without a controller loses stability. However, the application of battery-based angle feedback control exhibits its ability in enhancing transient stability, which validates Theorem 3, Theorem 5 and Remark 4. In Fig. 4, we plot the trajectories of battery power output change under three actuator saturation cases. Our novel control design is effective in managing the actuator saturation issue, which is consistent with Remark 3.

VIII. Conclusion

In this paper, we proposed a NNI systems framework for control of electrical power systems. Through the development of a new Lyapunov function fashioned in a manner reminiscent of the Luré-Postnikov form, we established a stability analysis for the feedback interconnection of a NNI system and a NNI controller. Additionally, we introduced a new class of NNI controllers to manage actuator saturation. Our results demonstrated that within this control framework, the controller eventually moved beyond the saturation boundary and the feedback system is locally stable in the sense of Lyapunov. This served as theoretical background supporting the application of battery-based control in electrical power systems. Validation through simulation results for single-machine-infinite-bus power systems further confirmed our results. Investigating large-scale power transmission networks will be a future research direction.

References

[1] A. Lanzon and I. R. Petersen, "Stability robustness of a feedback interconnection of systems with negative imaginary frequency response," *IEEE Transactions on Automatic Control*, vol. 53, no. 4, pp. 1042–1046, 2008.

[2] A. G. Ghallab and I. R. Petersen, "Negative imaginary systems theory for nonlinear systems: A dissipativity approach," *arXiv preprint arXiv:2201.00144*, 2022.

[3] K. Shi, I. R. Petersen, and I. G. Vladimirov, "Output feedback consensus for networked heterogeneous nonlinear negative-imaginary systems with free-body motion," *IEEE Transactions on Automatic Control*, vol. 68, no. 9, pp. 5536–5543, 2023.

[4] H. Bevrani, *Robust power system frequency control*. Springer, 2014, vol. 4.

[5] J. D. Glover, M. S. Sarma, and T. Overbye, *Power system analysis & design, SI version*. Cengage Learning, 2012.

[6] V. T. Tran, M. R. Islam, K. M. Muttaqi, and D. Sutanto, "An efficient energy management approach for a solar-powered EV battery charging facility to support distribution grids," *IEEE Transactions on Industry Applications*, vol. 55, no. 6, pp. 6517–6526, 2019.

[7] S. Borenstein, "It's time for rooftop solar to compete with other renewables," *Nature Energy*, vol. 7, no. 4, pp. 298–298, 2022.

[8] I. Višić, I. Strnad, and A. Marušić, "Synchronous generator out of step detection using real time load angle data," *Energies*, vol. 13, no. 13, p. 3336, 2020.

[9] Y. Chen, I. R. Petersen, and E. L. Ratnam, "Design and stability of angle based feedback control in power systems: A negative-imaginary approach," *arXiv preprint arXiv:2310.01781*, 2023.

[10] I. R. Petersen and A. Lanzon, "Feedback control of negative-imaginary systems," *IEEE Control Systems Magazine*, vol. 30, no. 5, pp. 54–72, 2010.

[11] J. Wang, A. Lanzon, and I. R. Petersen, "Robust cooperative control of multiple heterogeneous negative-imaginary systems," *Automatica*, vol. 61, pp. 64–72, 2015.

[12] J. Xiong, I. R. Petersen, and A. Lanzon, "A negative imaginary lemma and the stability of interconnections of linear negative imaginary systems," *IEEE Transactions on Automatic Control*, vol. 55, no. 10, pp. 2342–2347, 2010.

[13] W. M. Haddad and V. Chellaboina, *Nonlinear dynamical systems and control: a Lyapunov-based approach*. Princeton university press, 2008.

[14] J. Carrasco and W. P. Heath, "Comment on "Absolute stability analysis for negative-imaginary systems"[Automatica 67 (2016) 107–113]," *Automatica*, vol. 85, pp. 486–488, 2017.

[15] Y. Chen, K. Shi, I. R. Petersen, and E. L. Ratnam, "A nonlinear negative imaginary systems framework with actuator saturation for control of electrical power systems," *arXiv preprint arXiv:2311.06820*, 2023.